Supporting Information

Cedervall et al. 10.1073/pnas.1419906112

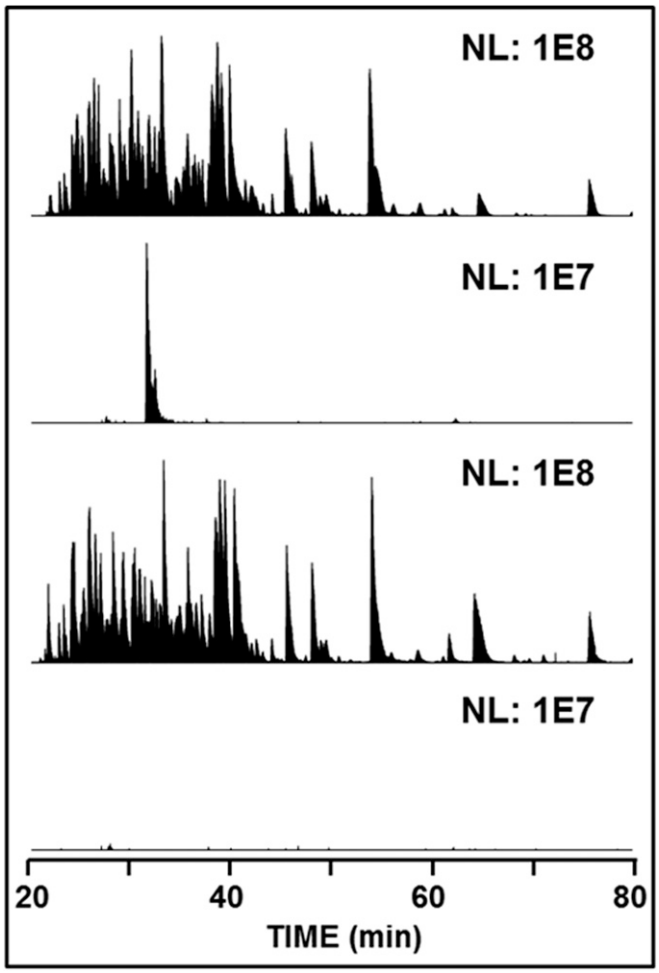

Fig. S1. LC-MS peptide mapping. Top, peptic digest of $PDE4B_{cryst}$ with no DTT treatment; second, extracted ion plot for $m/z = 789.615$, corresponding to $[M+4H]^{4+}$ of two peptide fragments (264-273 and 600–618) linked by a disulfide bond; third, DTT-treated peptic digest of $PDE4B_{cryst}$; and fourth, extracted ion plot as before for the DTT-treated sample. NL, normalized level. The reduced sample is a control as any peak identified as a disulfide linked fragment (second panel) is expected to be absent under reducing conditions (fourth panel). The identity of the DTT-sensitive fragment was confirmed by tandem-MS (Fig. S3).

Fig. S2. PDE4B$_{cryst}$ sequence coverage in LC-MS. Red font color indicates sequence covered by simple (i.e., not cross-linked) peptides detected in LC-MS on (*A*) nonreduced and (*B*) reduced peptic digest of PDE4B$_{cryst}$. Cys267 is highlighted in green and Cys610 is highlighted in teal. The cysteines were not detected in the nonreduced sample, but were detected in the reduced sample.

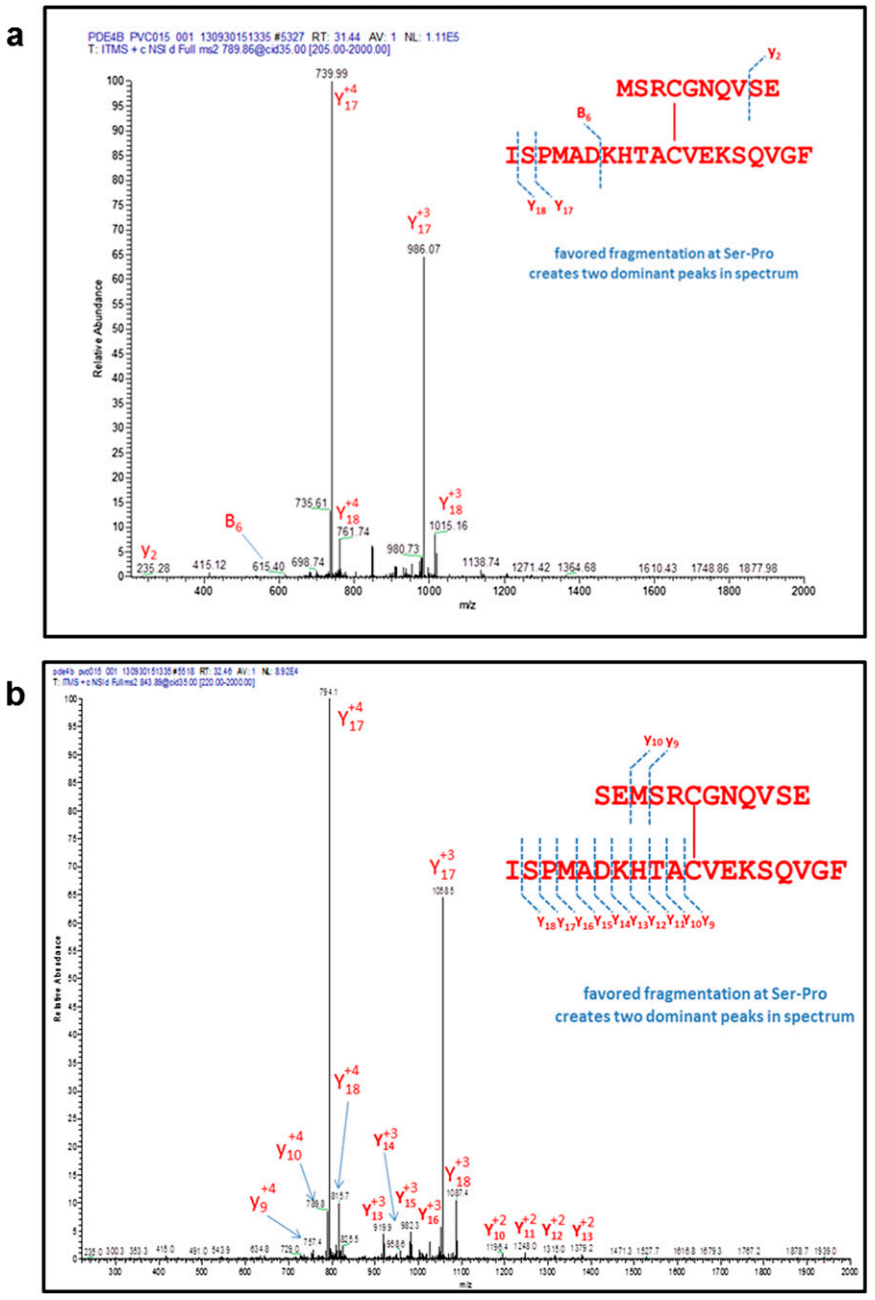

Fig. S3. Tandem MS spectrum (collision-induced dissociation) of (*A*) 4+ charged peak with *m/z* = 789.86 identified as the disulfide-linked fragment of $PDE4B_{cryst}$ linking peptides 264–273 and 600–618 (PDE4B1 numbering) and (*B*) 4+ charged peak with *m/z* = 843.89 identified as the fragment linking peptides 262–273 and 600–618. Major peaks in the spectrum support the identity assigned.

```
141 DYDLSPKAMSRNSSLPSEQHGDDLIVTPFAQVLASLRSVRNNFTILTNLHGT-SNKRSPA 199  Q07343 PDE4B
153 DYDMSPKTMSRNSSVTSEAHAEDLIVTPFAQVLASLRSVRSNFSLLTNVPVP-SNKRSPL 211  P27815 PDE4A
198 DYDLSPKSMSRNSSIASDIHGDDLIVTPFAQVLASLRTVRNNFAALTNLQDRAPSKRSPM 257  Q08499 PDE4D
127 DYELSPKAMSRNSSVASDLHGEDMIVTPFAQVLASLRTVRSNVAALARQQCLGAAKQGPV 186  Q08493 PDE4C

200 ASQPPVSRVNPQEESYQKLAMETLEELDWCLDQLETIQTYRSVSEMASNKFKRMLNRELT 259  Q07343 PDE4B
212 GGPTPVCKATLSEETCQQLARETLEELDWCLEQLETMQTYRSVSEMASHKFKRMLNRELT 271  P27815 PDE4A
258 CNQPSINKATITEEAYQKLASETLEELDWCLDQLETLQTRHSVSEMASNKFKRMLNRELT 317  Q08499 PDE4D
187 GNPSSSNQLPPAEDTGQKLALETLDELDWCLDQLETLQTRHSVGEMASNKFKRILNRELT 246  Q08493 PDE4C
```

Fig. S4. Sequence alignment of the dimerization domains in human PDE4A to -D. The conserved polar residues that make intrachain salt bridges in the crystal structure are highlighted in yellow, and the conserved hydrophobic residues that constitute the core of the 4-helix bundle that forms the primary dimer interface in $PDE4B_{cryst}$ are highlighted in red (UCR1) and green (UCR2). Sequence alignment was done in Uniprot.

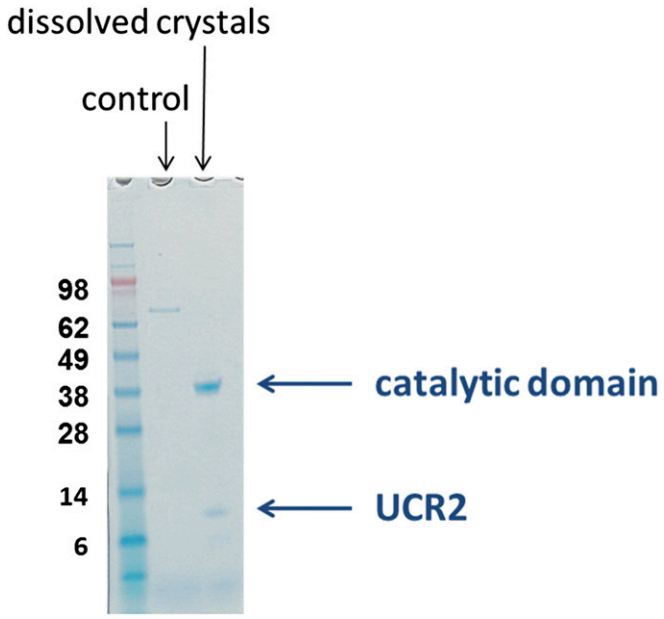

Fig. S5. Reducing SDS/PAGE analysis of dissolved PDE4B$_{cryst}$ crystals showed that proteolytic cleavage had occurred during crystallization. N-terminal sequencing and LC-MS analysis of the excised gel bands showed them to be catalytic domain (*Upper*) and UCR2 (*Lower*).

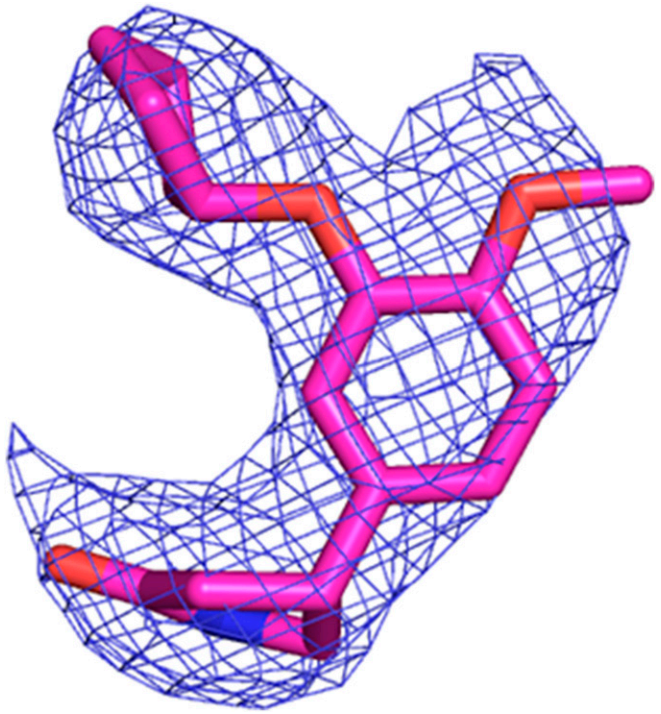

Fig. S6. Rolipram binding mode is well-defined in electron density maps. A (2*Fo-Fc*) map contoured at 1.4σ around rolipram in the PDE4B$_{cryst}$–rolipram complex crystal structure (resolution 3.2 Å).

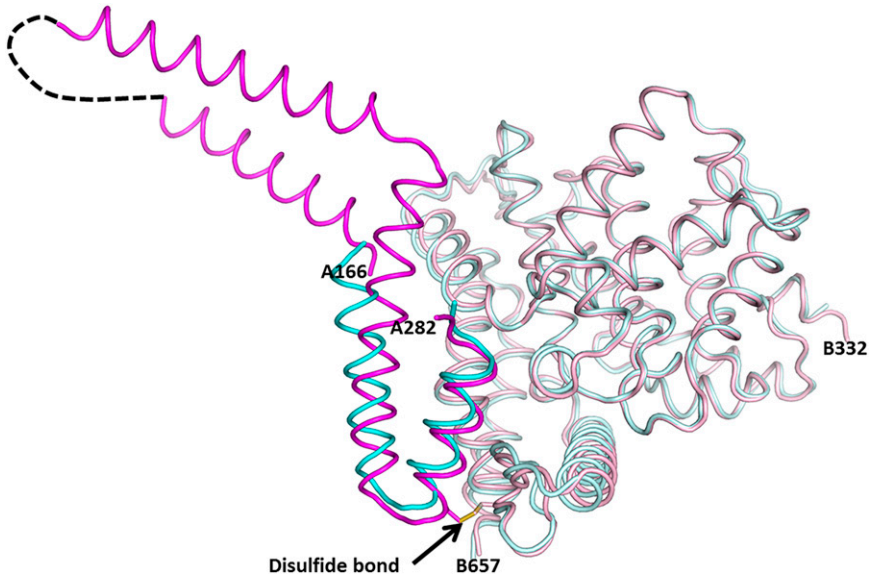

Fig. S7. Overlay of PDE4B$_{cryst}$ on PDB ID 3G45. PDE4B$_{cryst}$ is colored magenta and 3G45 is colored cyan with the catalytic domains of both proteins shown in lighter shades and the regulatory domains shown in darker shades. For PDE4B$_{cryst}$, the regulatory domain of subunit A (residues A166–A282) and the catalytic domain of subunit B (B332–B657) are shown. In this representation, the molecules have been superimposed to minimize the rmsd between Cα atoms of the catalytic domain (rmsd 0.68 Å calculated over all 335 Cα atoms of the catalytic domain). The disulfide bond between Cys267 and Cys610 in PDE4B$_{cryst}$ is labeled.

Table S1. Disulfide-linked peptide fragments of PDE4B$_{cryst}$ identified in peptic digest

Cys267-containing peptide*	Cys610-containing peptide*	$[M+4H]^{4+}$ theoretical†	$[M+4H]^{4+}$ observed†
262 SEMSR**C**GNQVSE 273	598 MEISPMADKHTA**C**VEKSQVGF 618	908.654	908.657
262 SEMSR**C**GNQVSE 273	600 ISPMADKHTA**C**VEKSQVGF 618	843.633	843.634
262 SEMSR**C**GNQVSE 273	605 DKHTA**C**VEKSQVGF 618	718.822	718.825
264 MSR**C**GNQVSE 273	598 MEISPMADKHTA**C**VEKSQVG 617	854.636	854.635
264 MSR**C**GNQVSE 273	600 ISPMADKHTA**C**VEKSQVGF 618	789.615	789.615

*Residue numbering follows sequence of PDE4B1 (UniProt accession Q07343): peptides listed in this Table include mutations S267C, C604A, and S610C. C267 and C610 are highlighted in bold font.
†Monoisotopic values are given for both theoretical and observed *m/z*.

Table S2. Thermodynamic parameters for rolipram binding to reduced and nonreduced PDE4B$_{cryst}$

PDE4B$_{cryst}$	Stoichiometry	K_D, nM	ΔG, kcal/mol	ΔH, kcal/mol	TΔS, kcal/mol
Reduced	0.83	55	−9.80	−16.54	−6.75
Nonreduced	0.90	101	−9.54	−15.60	−6.05

Table S3. List of mutations in *PDE4D* found in acrodysostosis patients, equivalent residues in PDE4B1 and numbering in Fig. 8

Number in Fig. 8	PDE4D*	PDE4B
1	Pro225Thr	Pro168
1	Pro225Leu	Pro168
2	Phe226Val	Phe169
2	Phe226Cys	Phe169
2	Phe226Ser	Phe169
3	Ala227Ser	Ala170
4	Gln228Glu	Gln171
5	Ser301Thr	Ser243
6	Met303Val	Met245
7	Ala304Val	Ala246
8	Val329Ala	Val271
9	Thr587Pro	Thr531
10	Glu590Ala	Glu534
11	Gly673Asp	Gly617
12	Ile678Thr	Ile622

*Data from ref. 1.

1. Lindstrand A, et al. (2014) Different mutations in PDE4D associated with developmental disorders with mirror phenotypes. *J Med Genet* 51(1):45–54.